Toward the computational rheometry of filled polymeric fluids

Wook Ryol Hwang* and Martien A. Hulsen[1]

*School of Mechanical and Aerospace Engineering, Research Center for Aircraft Parts Technology (ReCAPT),
Gyeongsang National University, Gajwa-dong 900, Jinju 660-701, Korea*
*[1]Department of Mechanical Engineering, Eindhoven University of Technology,
P.O. Box 513, 5600MB, Eindhoven, The Netherlands*

Abstract

We present a short review for authors' previous work on direct numerical simulations for inertialess hard particle suspensions formulated either with a Newtonian fluid or with viscoelastic polymeric fluids to understand the microstructural evolution and the bulk material behavior. We employ two well-defined bi-periodic domain concepts such that a single cell problem with a small number of particles may represent a large number of repeated structures: one is the sliding bi-periodic frame for simple shear flow and the other is the extensional bi-periodic frame for planar elongational flow. For implicit treatment of hydrodynamic interaction between particle and fluid, we use the finite-element/fictitious-domain method similar to the distributed Lagrangian multiplier (DLM) method together with the rigid ring description. The bi-periodic boundary conditions can be effectively incorporated as constraint equations and implemented by Lagrangian multipliers. The bulk stress can be evaluated by simple boundary integrals of stresslets on the particle boundary in such formulations. Some 2-D example results are presented to show effects of the solid fraction and the particle configuration on the shear and elongational viscosity along with the micro-structural evolution for both particles and fluid. Effects of the fluid elasticity has been also presented.

Keywords : direct numerical simulation, particle suspension, sliding bi-periodic frame, extensional bi-periodic frame, suspension rheology

1. Introduction

It is quite common to add particles to fluids and polymeric fluids in particular. The reasons can be quite diverse, e.g. for the manufacturing of ceramics where the polymer is removed after processing, changing the product properties (such as adding flame retardants), modifying the properties during processing, or even lowering the cost. Understanding the rheological behavior is necessary for processing those materials in a rational manner. In addition, the final properties of the product may also require certain rheological features or a specific suspension microstructure. Therefore, studying the rheological properties of particle-filled polymeric fluids is very important.

Understanding rheological properties of such a material is obviously very difficult, since they are determined by the flow-induced microstructure for both particles and the suspending fluid, such as clustering/alignment of particles or stretching and orientation of polymeric molecules. In order to understand the formation of such microstructures, one needs to fully consider hydrodynamic interaction between particles and fluids, inter-particle forces as well as complex rheological property of the fluid. Moreover, the inter-relationship between the microstructure and the bulk material behavior has not been clearly understood yet, especially for polymeric suspensions.

For a suspension of non-Brownian particles in a Newtonian fluid in simple shear flow, Brady and co-workers (e.g. Sierou and Brady, 2002) have shown that inclusion of hydrodynamic interactions using accelerated Stokesian dynamics results in a powerful numerical technique that can predict such a relationship between the microstructure and the macroscopic properties. However, as clearly indicated by Vermant and Solomon (2005), for suspensions of particles in rheologically more complex fluids, the developments of simulation methods that can accommodate the non-Newtonian nature of the suspending media is a necessary next step.

For recent couple of years, we have concentrated our research on the development of new computational methods that could satisfy the requirements above: i.e., direct numerical simulation techniques that give sufficiently accurate velocity (and its gradient) of the fluid medium along

*Corresponding author: wrhwang@gsnu.ac.kr

with full consideration of hydrodynamic and interparticular interactions and moreover that admit the usage of state-of-the-art viscoelastic constitutive models. In this paper, we present a short review of authors' work performed for this purpose (more specifically, Hwang et al., 2004a, 2004b, 2005; Hwang and Hulsen, 2006) on direct numerical simulations for inertialess particle suspensions, formulated either with a Newtonian fluid or with viscoelastic fluids, in both simple shear and planar elongational flows. In this paper, we restrict our discussion on non-Brownian hard particle suspension in two-dimensional flows.

The paper is organized as follows: in the next section, we start with mathematical treatment of freely suspended inertialess particles that can be well suited with the fictitious domain method. Then, we separately introduce bi-periodic domain concepts for simple shear and planar elongational flows, in order to construct the single representative cell problem for each flow. Subsequently, we discuss a method to incorporate the viscoelasticity of the fluid medium. In section 3, we present computational methods based on the combined weak formulation for each rheometric flow field along with proper implementation techniques. We will also present expressions for the bulk stress in such bi-periodic computational domain. Finally, we review several example results for both flows to illustrate the usefulness of the present scheme in predicting the bulk rheological properties and the microstructural evolution in particle suspensions in rheologically complex fluids.

2. Modeling aspects

2.1. Basic equations

As shown in Fig. 1, a representative rectangular domain, denoted by Ω, is the computational domain of this work and the four boundaries of the frame are denoted by Γ_i ($i=1, 2, 3, 4$). We use a symbol Γ for $\cup_{i=1}^{4} \Gamma_i$. Particles are denoted by $P_i(t)$ ($i=1, ..., N$) and N is the number of particles in a single domain. We use a symbol $P(t)$ for $\cup_{i=1}^{N} P_i(t)$,
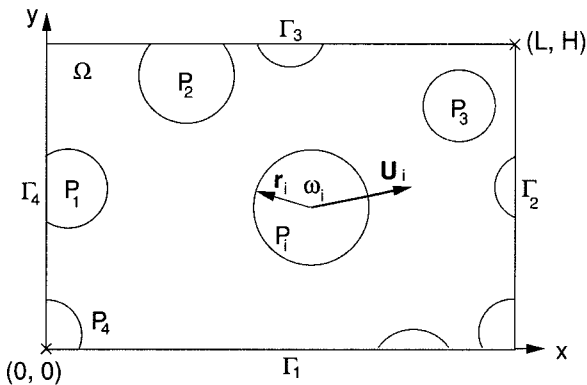

Fig. 1. A representative computational domain Ω with a small number of particles.

a collective region occupied by particles at a certain time t. For a particle P_i, $X_i=(X_i, Y_i)$, $U_i=(U_i, V_i)$, $\omega_i=\omega_i k$ and $\Theta_i =\Theta_i k$ are used for the coordinates of the particle center, the translational velocity, the angular velocity and the angular rotation, respectively; and k is the unit vector in the direction normal to the plane. Now we present the governing equations in a strong form for the Newtonian fluid medium for simplicity, neglecting inertia for both fluid and particles that can be usually accepted for suspension of small particles. The governing equation for particles will be discussed in the subsequent section and the extension to the viscoelastic flow will be presented in Sec. 2.5.

The set of equations for the fluid domain is given by

$$\nabla \cdot \sigma = 0, \text{ in } \Omega \backslash P(t), \tag{1}$$

$$\nabla \cdot u = 0, \text{ in } \Omega \backslash P(t), \tag{2}$$

$$\sigma = -pI + 2\eta D, \text{ in } \Omega \backslash P(t), \tag{3}$$

$$u = U_i + \omega_i \times (x - X_i) \text{ on } \partial P_i(t), (i=1, .., N). \tag{4}$$

Eqs. (1-4) are equations for the momentum balance, the continuity, the constitutive relation, and rigid-body conditions on particle boundaries, respectively. u, σ, p, I, D and η are the velocity, the stress, the pressure, the identity tensor, the rate of deformation tensor and the viscosity, respectively. Unknown rigid-body motions in Eq. (4) will be determined by hydrodynamic interactions.

2.2. Solid-liquid interaction

For the description of a particle in combination with fictitious domain methods, one can assign direct rigid-body motions on the region occupied by the particle (Glowinski et al., 1999; Yu et al., 2002), or impose zero rate-of-deformation over the region (Patankar et al., 2000). Both methods need domain discretization. However, we employ an alternative description for the particle domain instead for our work. We consider a circular particle as a rigid ring, which is filled with the same fluid as in the fluid domain so that the rigid-body condition is imposed on the particle boundary only. We call it the rigid-ring description. This description is possible, whenever inertia is negligible. The rigid-ring description needs discretization only along the particle boundaries so that it gives significant reduction on memory and it is easier to implement compared with methods using domain discretization. In addition, the boundary discretization allows the systematic treatment of boundary-crossing particles, which is important in bi-periodic simulations.

From the rigid-ring description, the governing equations for a region occupied by a particle P_i at a certain time t can be written as:

$$\nabla \cdot \sigma = 0, \text{ in } P_i(t), \tag{5}$$

$$\nabla \cdot u = 0, \text{ in } P_i(t), \tag{6}$$

$$\sigma = -pI + 2\eta D, \text{ in } P_i(t), \tag{7}$$

$$u = U_i + \omega_i \times (x - X_i), \quad \text{on } \partial P_i(t). \tag{8}$$

Eqs. (5-8) are the equations for the momentum balance, the continuity, the constitutive relation, and the boundary condition, respectively, which are exactly the same as fluid domain equations in Eqs. (1-4).

To determine the unknown rigid body motions (U_i, ω_i) of the particles, one needs balance equations for drag forces and torques on particle boundaries. In the absence of inertia and external forces or torques, particles are force-free and torque-free:

$$F_i = \int_{\partial P_i(t)} \sigma \cdot n \, ds = 0, \tag{9}$$

$$T_i = \int_{\partial P_i(t)} (x - X_i) \times (\sigma \cdot n) \, ds = 0, \tag{10}$$

where $T_i = T_i k$ and n is a normal vector on ∂P_i pointing out of the particle.

2.3. Simple shear flow

We consider flowing suspensions consisting of a large number of non-Brownian circular disk particles in a Newtonian fluid. Complex particle motions and hydrodynamic interactions induce complicated micro-structural developments. In order to deal with such problems, a well-defined bi-periodic domain needs to be introduced, through which one can observe what happens inside. The bi-periodic domain concept may transform a suspension in an unbounded domain with an infinite number of particles into a particulate flow problem in a unit cell which can be solved at reasonable computational costs. Ideally we want to translate the unit domain at the average velocity of the flow in a cell. In simple shear flows the Lees-Edwards boundary condition (LEbc), proposed by Lees and Edwards (1972) for Molecular Dynamics, satisfies the above requirements exactly, diminishing finite size effect of the computational domain.

We employ so-called the sliding bi-periodic frame, an extension of LEbc to the continuous field problem, in order to incorporate with the velocity-pressure formulation of the

finite element method. Fig. 2 shows sliding bi-periodic frames and a possible three-particle configuration in a single frame. At an arbitrary instance, say $t = 0$, an unbounded domain of interest can be regularly divided into an infinite number of frames of the width L and the height H. As time goes on, each frame translates along the shear direction at its own average velocity (of the flow inside the frame). Rows of the frames slide relatively to one another by an amount determined by the given shear rate $\dot{\gamma}$, elapsed time t and height of the frame H.

The amount of slide Δ between upper and lower frames is given by

$$\Delta = \dot{\gamma} H t. \tag{11}$$

For some properties of the sliding bi-periodic frame, refer to Hwang et al. (2004a). A sliding frame which contains a small number of particles can represent an infinite number of such systems because of the bi-periodicity as described in Fig. 2.

Now we consider mathematical descriptions of the bi-periodicity in the sliding frame (see Fig. 2). The kinematic relation and the force balance for the horizontal periodicity between Γ_2 and Γ_4 can be written as follows:

$$u(0, y) = u(L, y), \quad y \in [0, H] \tag{12}$$

$$t(0, y) = -t(L, y), \quad y \in [0, H], \tag{13}$$

where t are tractions on the boundaries.

The vertical sliding periodicity between Γ_1 and Γ_3 is more complicated, since it is time-dependent. One needs to take into account (i) coincidence in positions, (ii) the velocity continuity, and (iii) the force balance between Γ_1 and Γ_3. The two conditions for the vertical sliding periodicity can be summarized in turns as (for details, Hwang et al. 2004a):

$$u(x, H; t) = u(\{x - \dot{\gamma} H t\}^*, 0; t) + f, \quad x \in [0, L). \tag{14}$$

$$t(x, H; t) = -t(\{x - \dot{\gamma} H t\}^*, 0; t), \quad x \in [0, L). \tag{15}$$

$f = (\dot{\gamma} H, 0)$ originates from the difference in the x direc-
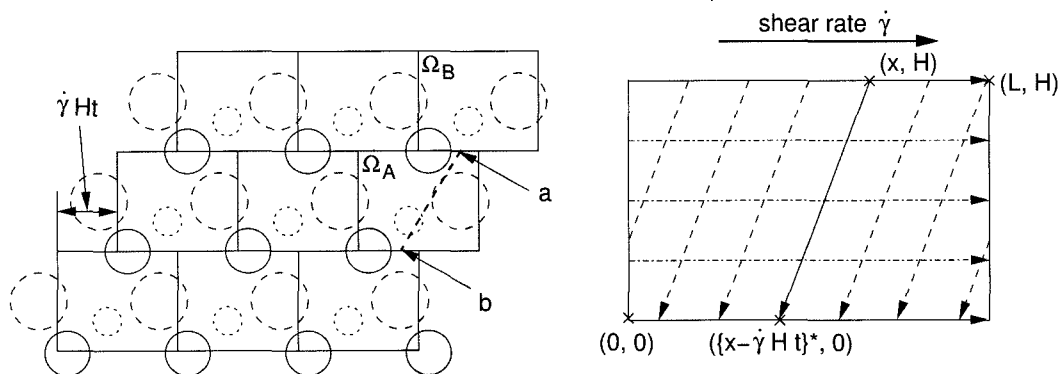

Fig. 2. A three-particle configuration of a sliding bi-periodic frame can represent a large number of repeated structures in simple shear flow (right). Kinematic relation for the vertical periodicity is present also (left) (Hwang et al., 2004a, 2004b).

tional velocity component; $\{\cdot\}^*$ denotes a modular function of L: e.g., $\{1.7L\}^* = 0.7L$ and $\{-1.7L\}^* = 0.3L$. Eqs. (12-15) complete the governing equation set for the fluid domain (with Eqs. 1-4).

2.4. Planar elongational flow

Now we consider suspensions in planar elongational flow. In non-equilibrium molecular dynamics simulation of elongational flow, Heyes (1985) introduced the concept of the deforming simulation cell, which is aligned in flow direction and stretches in that direction. The cross-flow dimensions of the cell decrease such that the volume of the cell remains constant. For planar elongational flows, it is possible to use so-called Kraynik-Reivelt boundary conditions (Kraynik and Reinelt, 1992) and simulations can performed indefinitely. However this approach is difficult to use and cannot be extended to uni-axial elongational or bi-axial stretching flows.

In order to introduce a bi-periodic domain for our work, we adopt the simple deforming cell approach of Heyes and propose the extensional bi-periodic frame as a computational domain for the representative unit cell problem in planar elongational flow of particle filled fluids.

Fig. 3 shows the extensional bi-periodic frames with the elongation rate $\dot{\varepsilon}$. (The coordinate system is indicated therein as well.) The extensional frame is a material frame in that it translates and deforms along the flow kinematics. The hatched region in Fig. 3 indicates a single frame for the illustration. At an arbitrary instance, say $t = 0$, the unbounded domain is regularly divided into an infinite number of cells (or frames) of the width L_0 and the height H_0. As time goes on, frames elongate in the horizontal direction and contract in the vertical direction, while translating along the flow. Given the elongation rate $\dot{\varepsilon}$ as in Fig. 2, the time-dependent changes of the width L and the height H of the frame can be expressed as

$$L(t) = L_0 \exp(\dot{\varepsilon}t), \quad H(t) = H_0 \exp(-\dot{\varepsilon}t). \tag{16}$$

Although each frame translates at different velocity, the frame dimensions $L(t)$ and $H(t)$ along with the relative velocity of the fluid particle with respect to the center of each frame are the same and periodic for all the extensional frames and for all time t. Also, such arguments are still valid for non-homogeneous fluid systems subject to planar elongational flow, e.g. particle suspensions or droplet emulsions, if the initial configuration of the particles or the droplets is periodic from the beginning. For details, refer to Hwang and Hulsen (2006).

Now we discuss the mathematical description of the bi-periodicity in the extensional frame. (In planar elongational flow, we use a computational domain centered at (0,0) for convenience. That is an extensional bi-periodic frame at a certain time t is given by $[-0.5L(t), 0.5L(t)] \times [-0.5H(t), 0.5H(t)]$). The continuity of the velocity field and the force balance need to be satisfied across the domain boundary Γ. The conditions in the horizontal direction (between Γ_2 and Γ_4) at a certain time t can be written as follows:

$$u(0.5L(t), y) = u(-0.5L(t), y) + f_h, \ y \in [-0.5H(t), 0.5H(t)] \tag{17}$$

$$t(0.5L(t), y) = -t(-0.5L(t), y), \ y \in [-0.5H(t), 0.5H(t)], \tag{18}$$

where the vector t is the traction force on the boundary and $f_h = (\dot{\varepsilon}L(t), 0)$. With the elongation rate $\dot{\varepsilon}$, the velocity in the x direction on the right boundary (Γ_2) is faster than that on the left boundary (Γ_4) by the amount of the velocity difference $\dot{\varepsilon}L(t)$. Similarly, the conditions for the periodicity in the vertical direction between Γ_1 and Γ_3 are

$$u(x, 0.5H(t)) = u(x, -0.5H(t)) + f_v, \ x \in [-0.5L(t), 0.5L(t)] \tag{19}$$

$$t(x, 0.5H(t)) = -t(x, -0.5H(t)), \ x \in [-0.5L(t), 0.5L(t)]. \tag{20}$$

The velocity difference in the vertical direction is specified by $f_v = (0, -\dot{\varepsilon}H(t))$ in Eq. 19. Again Eqs. (17-19) complete
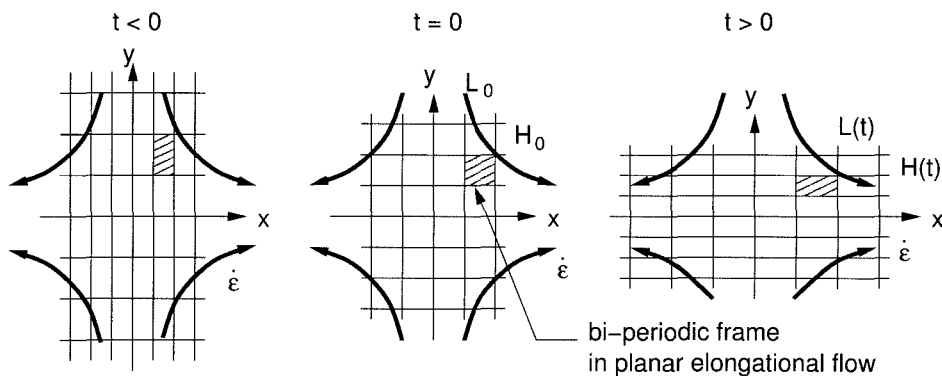
Fig. 3. Extensional bi-periodic frames in planar elongational flow. The movement and the deformation of a single frame is indicated for the illustration (hatched) (Hwang and Hulsen, 2006).

the governing equation set for the fluid domain (with Eqs. 1-4) for particle suspensions in planar elongational flow.

2.5. Viscoelasticity

Although modeling up until now has been carried out for particle suspensions in a Newtonian fluid, one can easily extend it to cover the viscoelastic fluid medium case. Since details on this issue have been discussed in Hwang *et al.* (2004b), we briefly summarize additional consideration necessary to accommodate the viscoelasticity in the fluid here.

Consider a simple non-linear viscoelastic constitutive model (Oldroyd-B) in fluid domain:

$$\sigma = -p\boldsymbol{I} + 2\eta_s \boldsymbol{D} + \tau_p, \quad \text{in } \Omega \backslash P(t), \tag{21}$$

where $\boldsymbol{I}$, τ_p, η_s, η_p and λ are the identity tensor, the polymeric contribution to the extra-stress tensor, the viscosity of a Newtonian solvent, the polymer viscosity and the relaxation time, respectively. The symbol $\overset{\triangledown}{}$ denotes the upper-convected time derivative, defined as

$$\overset{\triangledown}{\tau_p} \equiv \frac{\partial \tau_p}{\partial t} + \boldsymbol{u} \cdot \nabla \tau_p - (\nabla \boldsymbol{u})^T \cdot \tau_p - \tau_p \cdot \nabla \boldsymbol{u}.$$

We remark that, even with the elasticity of fluid, the rigid-ring description (Sec. 2.2) is still valid. Indeed, the description holds whenever inertia for both fluid and particle are negligible and this means that a particle is considered as a rigid ring, which is filled with the same fluid as in the fluid domain. Therefore, Eq. (21) holds for the domain occupied by the particle also, along with the remaining Eqs. (5-8). The initial condition for the polymer stress is the stress-free state, as it should be inside the rigid-ring and we do not need an inflow condition for the polymer stress τ_p, since there is no net convection of material particles across the particle boundary.

3. Computational methods

3.1. Combined weak formulation

We follow the approach of Glowinski *et al.* (1999) in the derivation of the weak form in the sense that fluid-particle interactions are treated implicitly via the combined weak formulation where hydrodynamic force and torque on a particle boundary exactly cancel. However, we will make a few modifications for the rigid-ring description of particles (Eqs. 5-8) and for the bi-periodic frame constraints: Eqs. (12) and (14) for the sliding bi-periodic frame, and Eqs. (17) and (19) for the extensional bi-periodic frame (Hwang *et al.*, 2004a, 2005a; Hwang and Hulsen 2006).

We introduce three different kinds of Lagrangian multipliers λ^h, λ^v, and $\lambda^{p,i}$, which are associated with the kinematic constraint equation for the periodicity in the horizontal direction (Eq. 12 for simple shear flow or Eq. 17 for planar elongational flow), the constraint equation for

periodicity in the vertical direction (Eq. 14 for simple shear flow or Eq. 19 for planar elongational flow) and the rigid-ring constraint equation along the i-th particle boundary (Eqs. 4 and 8):

$$\boldsymbol{\lambda}^h = (\lambda_x^h, \lambda_y^h) \in L^2(\Gamma_4)^2,$$
$$\boldsymbol{\lambda}^v = (\lambda_x^v, \lambda_y^v) \in L^2(\Gamma_3)^2,$$
$$\boldsymbol{\lambda}^{p,i} = (\lambda_x^{p,i}, \lambda_y^{p,i}) \in L^2(\partial P_i(t))^2.$$

In Hwang *et al.* (2004a), we showed that the multipliers λ^h and λ^v are the traction force on the domain boundary Γ and that the multiplier $\lambda^{p,i}$ is related to the traction force acting on the particle boundary $\partial P_i(t)$. This can be considered quite useful in evaluating the bulk stress, without introducing the domain integral.

Below is presented the combined weak formulation for Newtonian particle suspensions in sliding bi-periodic frame of simple shear flow, as an example. Application to extensional bi-periodic frame for planar elongational flow and that for the viscoelastic fluid medium will be discussed in the next subsection:

Find $\boldsymbol{u} \in H^1(\Omega)^2$, $\boldsymbol{U}_i \in \mathbb{R}^2$, $\omega_i \in \mathbb{R}$, $\boldsymbol{\lambda}^{p,i} \in L^2(\partial P_i(t))$, $p \in L^2(\Omega)$, $\boldsymbol{\lambda}^h \in L^2(\Gamma_4)$, and $\boldsymbol{\lambda}^v \in L^2(\Gamma_3)$ $(i=1, .., N)$ such that

$$-\int_\Omega p\nabla \cdot \boldsymbol{v} dA + \int_\Omega 2\eta \boldsymbol{D}(\boldsymbol{u}) : \boldsymbol{D}(\boldsymbol{v}) dA$$

$$+\sum_i^N \langle \boldsymbol{\lambda}^{p,i}, \boldsymbol{v} - (\boldsymbol{V}_i + \chi_i \times (\boldsymbol{x}-\boldsymbol{X}_i)) \rangle_{\partial P_i} \tag{22}$$

$$+\langle \boldsymbol{\lambda}^v, \boldsymbol{v}(x, H; t) - \boldsymbol{v}(\{x-\dot{\gamma}Ht\}^*, 0; t) \rangle_{\Gamma_3}$$

$$+\langle \boldsymbol{\lambda}^h, \boldsymbol{v}(0, y) - \boldsymbol{v}(L, y) \rangle_{\Gamma_4} = 0$$

$$\int_\Omega q\nabla \cdot \boldsymbol{u} dA = 0, \tag{23}$$

$$\langle \boldsymbol{\mu}^{p,i}, \boldsymbol{u} - (\boldsymbol{U}_i + \omega_i \times (\boldsymbol{x}-\boldsymbol{X}_i)) \rangle_{\partial P_i} = 0, \quad (i=1, .., N), \tag{24}$$

$$\langle \boldsymbol{\mu}^h, \boldsymbol{u}(0, y) - \boldsymbol{u}(L, y) \rangle_{\Gamma_4} = 0, \tag{25}$$

$$\langle \boldsymbol{\mu}^v, \boldsymbol{u}(x, H; t) - \boldsymbol{u}(\{x-\dot{\gamma}Ht\}^*, 0; t) \rangle_{\Gamma_3} = \langle \boldsymbol{\mu}^v, \boldsymbol{f} \rangle_{\Gamma_3}, \tag{26}$$

for all $\boldsymbol{v} \in H^1(\Omega)^2$, $\boldsymbol{V}_i \in \mathbb{R}^2$, $\chi_i \in \mathbb{R}$, $q \in L^2(\Omega)$, $\boldsymbol{\mu}^{p,i} \in L^2(\partial P_i(t))$, $\boldsymbol{\mu}^h \in L^2(\Gamma_4)$, and $\boldsymbol{\mu}^v \in L^2(\Gamma_3)$ $(i=1, .., N)$. The inner product $\langle \cdot , \cdot \rangle_{\Gamma_j}$ is the standard inner product in $L^2(\Gamma_j)$:

$$\langle \boldsymbol{\mu}, \boldsymbol{v} \rangle_{\Gamma_j} = \int_{\Gamma_j} \boldsymbol{\mu} \cdot \boldsymbol{v} \, ds.$$

3.1.1. Remarks

1. Force-free, torque-free rigid-body motions of particles are satisfied in a weak sense through rigid-ring constraints (Eqs. 22 and 24); and the Lees-Edwards boundary condition is combined with the weak form through the sliding bi-periodic frame constraints (Eqs. 22, 25 and 26).

2. Once a particle configuration is given, one can solve Eqs. (22-26), to get the solution $(\boldsymbol{u}, p, \boldsymbol{U}_i, \omega_i)$ and all the Lagrangian multipliers, and then determine the next particle configuration.

3. It is necessary to specify a reference velocity at a single point in the fluid domain, since the sliding boundary constraints give only relative difference in velocities of the boundaries. To obtain a simple shear flow in the x direction, the y component of the reference velocity needs to be specified zero.

4. The pressure level should be specified through one of the normal components of the Lagrangian multipliers on Γ to the boundary (i.e., λ_x^h or λ_y^v), since the Lagrangian multiplier is a traction.

3.1.2. Planar elongational flow

The weak form (Eqs. 22-26) can be modified for planar elongational flow, simply by replacing the weak equations (Eqs. 25 and 26) for the sliding bi-periodic frame by those for the extensional bi-periodic frame as follows:

$$\langle \mu^h, \, u(-0.5L, \, y) - u(0.5L, \, y) \rangle_{\Gamma4} = \langle \mu^x, \, f_h \rangle_{\Gamma4}, \, f_h = (\dot{\varepsilon}L(t), \, 0) \tag{27}$$

$$\langle \mu^y, \, u(x, \, 0.5H) - u(x, \, -0.5H) \rangle_{\Gamma3} = \langle \mu^y, \, f_v \rangle_{\Gamma3}, \, f_v = (0, \, -\dot{\varepsilon}H(t)) \tag{28}$$

The corresponding variational term should be present in the weak equation for the momentum balance (Eq. 22) as below:

$$- \int_\Omega p\nabla \cdot v \mathrm{d}\Omega + \int_\Omega 2\eta D(u) \, : \, D(v)\mathrm{d}\Omega + \sum_{i=1}^{N} \langle \lambda^{p,i},$$

$$v - [V_i - \chi_i k \times (x - X_i)] \rangle_{\partial P_i} + \langle \lambda^h, \, v(-0.5L, \, y) - v(0.5L, \, y) \rangle_{\Gamma4}$$

$$+ \langle \lambda^v, \, v(x, \, 0.5H) - v(x, \, -0.5H) \rangle_{\Gamma3} = 0 \tag{29}$$

Again the extensional bi-periodic frame constraint is satisfied weakly with the multipliers λ^h and λ^v(Eqs. 29, 27 and 28). For details on the weak form in this case, refer to Hwang and Hulsen (2006).

3.1.3. Viscoelastic fluid medium

Below we briefly describe the extension of the previous weak form to incorporate the viscoelastic fluid. We employ the DEVSS method, a mixed finite-element formulation developed by Guénette and Fortin (1995), which appears to provide one of the most robust formulations currently available. The DG formulation of Fortin and Fortin (1989) is used for the discretization of the constitutive equation. The combination of the DEVSS formulation with DG has been verified to produce a remarkably stable solution, in particular, for flows with a geometrical singularity (Baaijens 1998).

For the DEVSS formulation, we introduce an extra variable e, the viscous polymer stress.

$$e = 2\eta_p D. \tag{30}$$

Then one can rewrite the momentum equations for the fluid domain (Eq. 1) and for the particle domain (Eq. 5) with the viscous polymer stress, which gives extra stability in the discretized equations compared with the formulation without e.

The weak form for the viscous polymer e in DEVSS is

$$- \int_\Omega e_s \, : \, D[u]\mathrm{d}A + \frac{1}{2\eta_p} \int_\Omega e_s \, : \, e\mathrm{d}A = 0, \tag{31}$$

and the evolution of the viscoelastic stress τ_p can be evaluated by DG:

$$\int_\Omega S \, : \, (\lambda \overset{\triangledown}{\tau}_p + \tau_p - 2\eta_p D[u])\mathrm{d}A + \lambda \sum_e \int_{\Gamma_e^{in}} S \, : \, (\tau_p - \tau_p^{ext})(u \cdot n)\mathrm{d}s = 0. \tag{32}$$

In Eqs. (31) and (32), e_s and S are tensorial test functions. In Eq. (32), n is the unit outward normal vector on the boundary of element e, Γ_e^{in} is the part of the boundary of element e where $u \cdot n < 0$, and τ_p^{ext} is the polymer stress in the neighboring upwind element.

The DG method, which uses discontinuous interpolation of the polymer stress, is particularly suited in this simulation not only because of minimal coupling between elements, avoiding a large number of coupled equations, but also from the inherent discontinuous nature of the fictitious domain method, since the viscoelastic stress is discontinuous across the particle boundary.

3.2. Implementation

For the discretization of the momentum equation in the weak form, we use regular quadrilateral elements with continuous bi-quadratic interpolation (Q_2) for the velocity u, discontinuous linear interpolation (P_1) for the pressure p for the entire computational domain, including the interior of the particle. An example mesh for the two particle problem is presented in Fig. 4.

To discretize the weak form of the rigid-ring constraint, we use the point collocation method. For example, the integral in Eq. (24) has been approximated as follows:

$$(\mu^{p,i}(x'), \, u(x') - \{U_i + \omega_i \times (x - X_i)\})_{\partial P_i}$$

$$\approx \sum_{k=1}^{M_i} \mu_k^{p,i} \cdot \{u(x'_k) - (U_i + \omega_i \times (x_k - X_i))\}, \tag{33}$$

where M_i, x_k, x'_k and $\mu_k^{p,i}$ are the number of the collocation points on P_i, the original (before relocation) of the k-th col-
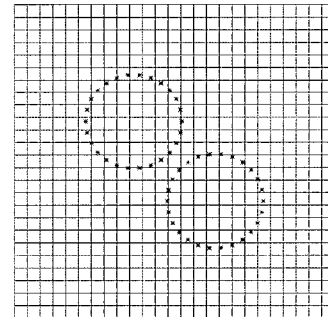

Fig. 4. An example finite-element mesh. Particles are described by the points collocated on the particle boundary.

location point, the relocated coordinate of the k-th collocation point and the collocated Lagrangian multiplier at x'_k, respectively. Approximately one collocation point in an element appears to give the most accurate solution (Hwang et al., 2004a).

To discretize the boundary integrals for the horizontal and vertical periodicity for both simple shear and planar elongational flows, we use the mortar element method. If the corresponding elements to be attached are conforming, the nodal collocation method will be the best method, since it does not introduce any approximation. Otherwise, the mortar element method in the integral expression is necessary to guarantee the continuous attachment for both velocity field and traction force. In our experience, the continuous linear interpolation of the Lagrangian multipliers renders the best result for non-conforming elements (Seshaijer and Suri 2000; Hwang et al., 2004a). Since the facing elements between Γ_2 and Γ_4 or between Γ_1 and Γ_3 are always conforming due to the regular discretization of the computational domain, one could use the nodal collocation method to implement the periodicity constraint for both directions. The latter method found to generate identical results with the method used in this work.

3.3. Bulk stress expression

The bulk stress, the average stress over the domain, can be expressed, for a volume V, as the sum of the fluid contribution and the particle contribution (Batchelor 1970):

$$\langle \sigma \rangle = \frac{1}{V}\int_V \sigma \, dV = \frac{1}{V}\int_{V_f} \sigma \, dV + \frac{1}{V}\int_{V_p} \sigma \, dV,$$

where $\langle \cdot \rangle$ denotes the averaged quantity in V, V_f and V_p are the volume occupied by the fluid and the particle, respectively. In the weak formulation of the sliding bi-periodic frame, we have the boundary integral expression for the bulk stress using the identity between the traction force and the Lagrangian multipliers λ^h, λ^v and λ^p, by comparing the standard weak form under prescribed tractions on Γ with the weak form of the momentum balance (Eq. 22). (For details, refer to Hwang et al., 2004a)

The Lagrangian multipliers λ^h and λ^v for the sliding bi-periodic frame constraints in the weak form (Eqs. 25 and 26) can be identified by the traction force t on the domain boundary Γ, by comparing the standard weak form under prescribed tractions on Γ with the weak form of the momentum balance (Eq. 22). Using the identity, the bulk stress over the computational domain can be expressed by boundary integrals of the Lagrangian multipliers along Γ:

$$\langle \sigma_{11} \rangle = \frac{1}{A_f}\int_0^L (\{x - \dot{\gamma}Ht\}^* - x)\lambda_x^v(x)dx + \frac{1}{H}\int_0^H \lambda_x^h(y)dy, \quad (34a)$$

$$\langle \sigma_{22} \rangle = -\frac{1}{L}\int_0^L \lambda_y^v(x)dx, \quad (34b)$$

$$\langle \sigma_{12} \rangle = \frac{1}{A_f}\int_0^L (\{x - \dot{\gamma}Ht\}^* - x)\lambda_y^v(x)dx + \frac{1}{H}\int_0^H \lambda_y^h(y)dy$$

$$= -\frac{1}{L}\int_0^L \lambda_x^v(x)dx. \quad (34c)$$

Since such a relationship is still valid in the extensional bi-periodic frame, one can find similar expression for the bulk stress in extensional bi-periodic frame in Hwang and Hulsen (2006). Also, the same relationship is valid in the viscoelastic flow, since the traction force includes the contribution from the polymer stress, $t = n \cdot (-p\mathbf{I} + 2\eta_s \mathbf{D} + \tau_p)$. One can use Eq. (34) as is for the viscoelastic suspensions.

4. Some results

4.1. Simple shear flow

The first review problem is stated as follows: a single particle of radius r is suspended freely at a center of a sliding bi-periodic frame of size 1×1 under three different shear rate $\dot{\gamma} = 0.1$, 1 and 2 in an Oldroyd-B fluid of the Newtonian solvent viscosity $\eta_s = 1$ and the polymer viscosity $\eta_p = 1$. The relaxation time λ is 0.5. The reference velocity has been specified zero at the center of the left boundary so that the particle does not translate relatively to the frame, but rotates at the fluctuating angular velocity. This problem represents a regular configuration of an infinite number of such a particle system and the initial configuration is reproduced after the period $T = L/(\dot{\gamma}H)$.

By taking the time average from steady oscillation parts of the bulk stress result, one can obtain steady time-averaged bulk suspension properties, as shown in Fig. 5 as a function of solid area fraction and the Weissenberg number. The bulk viscosity and the first normal stress coefficient show the shear-thickening behavior. For a small Weissenberg number (We = 0.05), the shear viscosity converges to that of Newtonian system and for the small value of solid area fraction ϕ the shear viscosity converges to Einstein's analytic results for a dilute Newtonian system with the coefficient 2 (Brady, 1984). Also the steady averaged first normal stress coefficient converges to 1 of pure Oldroyd-B fluid for small value of ϕ and it converges to the second-order fluid (SOF) limit for a small Weissenberg number (We = 0.05) and for a small value of ϕ (Patankar and Hu 2001).

Regarding bulk suspension behavior, one common experimental observation is that the first normal stress difference in a filled viscoelastic fluid is a power-law function of the imposed shear stress such that $N_1 \approx \tau^n$ with an exponent n that appears to depend on the specific matrix fluid used in preparing the suspensions (Tanaka and White, 1980; Ohl and Gleissle, 1993; Mall-Gleissle et al., 2002). With this argument, the n value in the Oldroyd-B fluid becomes 2, since it is independent of the volume fraction. In order to check the appearance of such a relationship in
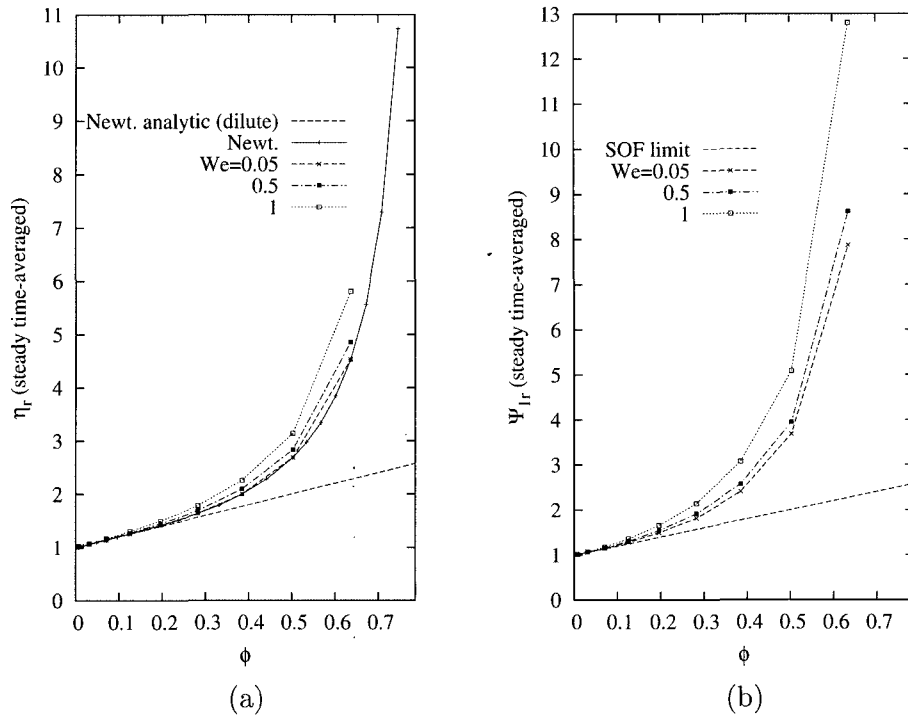
Fig. 5. The steady time-averaged bulk suspension properties as a function of the solid area fraction ϕ for different Weissenberg numbers $\phi_{max} = \pi/4$). (a) The relative shear viscosity and (b) the relative first normal stress difference coefficient. (Reproduced from Hwang *et al.*, 2004b).
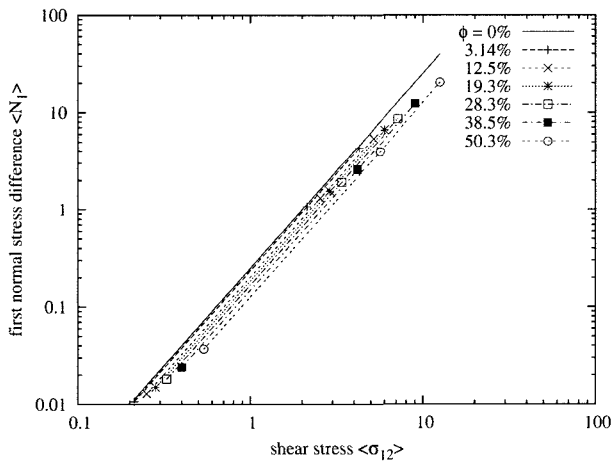
Fig. 6. The scaling between the steady time-averaged first normal stress difference and the shear stress in suspensions formulated with an Oldroyd-B fluid for various solid area fraction $\phi(\eta_p = \eta_s = 1)$. (Reproduced from Hwang *et al.*, 2004b).

our simulation results, we plotted the steady time-averaged first normal stress difference as a function of the steady bulk shear stress using the log-log scale in Fig. 6. Interestingly, our single-particle simulations in a 2-D sliding frame reveal a set of parallel straight lines which gradually shift to the shear stress axis with increasing solid area frac-

tions, for the wide range of ϕ, from the low particle concentration (3.14%) to the extremely high concentration (50.3%). For further analysis results on this example, refer to Hwang *et al.* (2004b).

As for the second example of simple shear flow, six randomly distributed particles in the sliding bi-periodic frame. The main objective here is to see how complicated particle/ fluid and particle/particle interactions affect the microstructural behavior in concentrated suspensions with a viscoelastic fluid. The size of the sliding frame is 1 × 1 and the solid area fraction $\phi = 0.296$. Fig. 7 shows the instantaneous distributions of the trace of tensor A:

$$A = I + \frac{\lambda}{\eta_p} \tau_p.$$

Firstly, one can observe strong elongational flows generated between separating particles. Secondly, another high stretched region occurs when two particles approach (or kiss) each other closely. Thirdly, there is also weak elongational flow region between particles aligned parallel to the flow direction. The value of tr(A) in such a region is sometimes lower than the value 2.5, which is the value of the pure Oldroyd-B fluid under the same condition. Therefore, the resultant microstructure becomes highly non-uniform and anisotropic. Especially, there seems to be a typical orientation for the highly stretched regions which originate from separating particles. The presence of the ori-
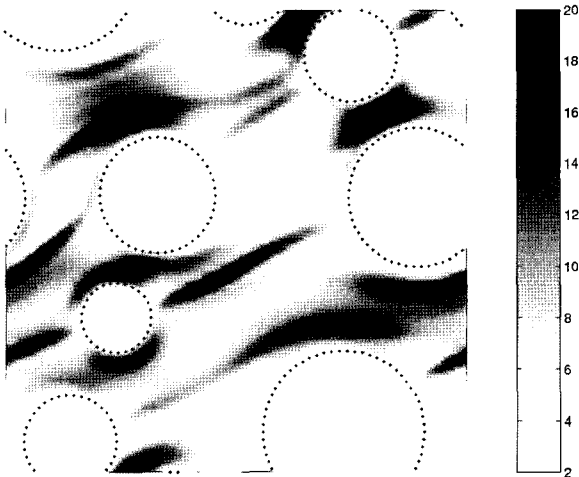
178

Fig. 7. The distribution of the trace of the conformation tensor in the six particle problem with different radii with We=1 at $\dot{\gamma}t(=t/\lambda)=6.384$. (Reproduced from Hwang et al., 2004b).

Fig. 8. An example 100 particle problem result for $r=0.025$. The plotted quantity is the distribution of the shear rate II_{2D}: $\dot{\varepsilon}t$ = 0, 0.5 and 1 (from the top to the bottom). (Reproduced from Hwang and Hulsen, 2006).

ented highly elongational flows is particularly interesting, since it induces polymer molecules to align in such a direction, which could affect the micro-rheological behavior of the suspension. (Refer to Schrauwen et al. (2002) for experimental observations about flow effects on the impact toughness in the injection-molded products of a hard particle-filled semi-crystalline polymer.)

4.2. Planar elongational flow

We review one example problem here for suspensions in planar elongational flow: randomly distributed 100 particles of the same radius r are suspended initially in an extensional bi-periodic frame of $L_0=H_0=1$ under the given elongation rate $\dot{\varepsilon}=1$ and the fluid viscosity $\eta=1$.

Fig. 8 shows an example result with a particle radius $r= 0.025$ ($\phi=0.196$) for the strain $\dot{\varepsilon}t=0$, 0.5 and 1 with the distribution of the total shear rate (II_{2D}). In this case, the vertical distances between particles decrease exponentially, while the horizontal distance increases, due to the planar elongational flow. However, there is no vertical alignment of particles, since randomly distributed particles and their interactions always keep the particles from being aligned: particles continuously fill in the space between the exponentially separating other particles. Therefore, one can expect limited increase of the bulk elongational viscosity with respect to the applied strain in many particle problems. Plotted in Fig. 9 is the relative bulk elongational viscosity computed in the 100 particle problems of several different solid area fraction ϕ with respect to the extensional strain ε. The average horizontal distance slightly increases and the average vertical distance slightly decreases as a function of strain. This means that the particle distribution becomes slightly anisotropic, which can also be noticed in Fig. 8. We believe that the anisotropic
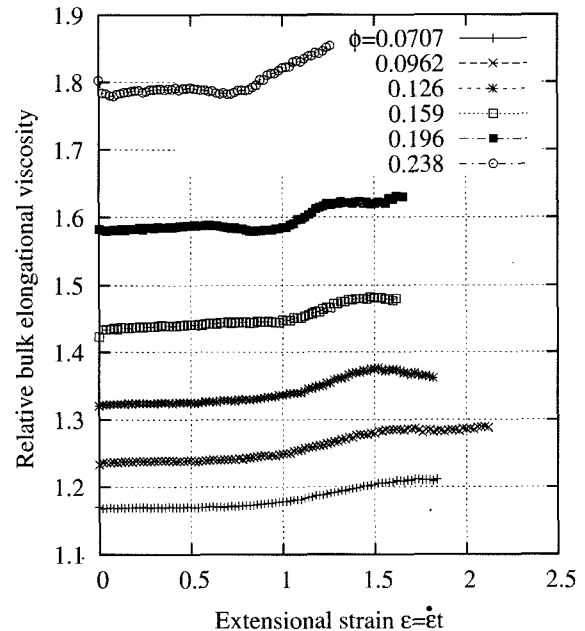

Fig. 9. The bulk relative elongational viscosity $\bar{\eta}_{1r}$ of the 100 particle problems as a function of the extensional strain ε = $\dot{\varepsilon}t$ for several values of the solid area fraction ϕ. (Reproduced from Hwang and Hulsen, 2006).

distribution here explains the slight increase in elongational viscosity as a function of strain. (For more details of analysis with other examples, refer to Hwang and Hulsen (2006).)

5. Conclusions and future works

In this work, we present a review for the authors' previous works (Hwang et al., 2004a; 2004b; 2005; Chung et al., 2005; Hwang and Hulsen, 2006) on direct numerical

simulations for inertialess hard particle suspensions formulated either with a Newtonian fluid or with viscoelastic polymeric fluids to understand the microstructural evolution and the bulk material behavior. In our work, we employ two well-defined bi-periodic domain concepts such that a single cell problem with a small number of particles may represent a large number of repeated structures: one is the sliding bi-periodic frame for simple shear flow and the other is the extensional bi-periodic frame for planar elongational flow. Main features of our direct simulation method can be summarized as follows:

- for simple shear flow, the sliding bi-periodic frame concept of Lees and Edwards (1972) for discrete particles has been extended to continuous fields and combined with the velocity-pressure formulation of the fictitious-domain/finite-element method;
- for planar elongational flow, the extensional bi-periodic frame concept of Heyes (1985) has been combined with the velocity-pressure formulation of the fictitious-domain/finite-element method;
- inertialess particles are described by their boundaries only (the rigid-ring description), eliminating domain discretization of particles, which allows general treatments of boundary-crossing particles;
- for accurate and stable computation of viscoelastic flows, the sliding bi-periodic domain concept has been combined with the DEVSS/DG finite-element method.

With this numerical scheme, we have attempted to understand the formation of microstructure, which is determined by complex rheology of the fluid medium and hydrodynamic interaction between fluid and particles, and its inter-relationship with the bulk rheogical properties of particle suspensions. Concentrating on 2-D circular disk particles, we discussed the bulk rheology of the suspensions and the micro-structural developments through the review of three numerical examples: the first one is for single particle in an Oldroyd-B fluid in sliding bi-periodic frame, the second is for six particles in the same fluid in sliding bi-periodic frame, and the last one for 100 particles problem in an extensional bi-periodic frame. In fact, the present scheme can be easily applied to 3-D problems without any significant modification and some preliminary results on this can be found in Hwang et al. (2004c). It can also be extended non-circular/non-spherical particle suspensions and some preliminary results on elliptic particle suspensions can be found in Chung et al. (2005).

Acknowledgement

References

Baaijens, F.P.T., 1998, Mixed finite element methods for viscoelastic flow analysis: a review, *J. Non-Newtonian Fluid Mech.* **79**, 361-385.

Batchelor, G.K., 1970, The stress system in a suspension of force-free particles *J. Fluid Mech.* **41**, 545-570.

Brady, J.F., 1984, The Einstein viscosity correction in n dimensions, *Int. J. Multiphase Flow* **10**, 113-114

Chung, H.T., S.H. Kang and W.R. Hwang, 2005, Numerical simulations of elliptic particle suspensions in sliding bi-periodic frames, *Korea-Australia Rheol. J.* **17**, 171-180.

Fortin, M. and A. Fortin, 1989, A new approach for the FEM simulation of viscoelastic flows, *J. Non-Newtonian Fluid Mech.* **32**, 295-310.

Glowinski, R., T.-W. Pan, T.I. Hesla and D.D. Joseph, 1999, A distributed Lagrangian multiplier/fictitious domain method for particulate flows, *Intern. J. Multiphase Flows* **25**, 755-749.

Guénette, R. and M. Fortin, 1995, A new mixed finite element method for computing viscoelastic flows, *J. Non-Newtonian Fluid Mech.* **60**, 27-52.

Heyes, D.M., 1985, Molecular dynamics simulations of extensional, sheet and unidirectional flow, *Chemical Physics* **98**, 15-27.

Hwang, W.R., M.A. Hulsen and H.E.H. Meijer, 2004a, Direct simulation of particle suspensions in sliding bi-periodic frames, *J. Comput. Phys.* **194**, 742-772.

Hwang, W.R., M.A. Hulsen and H.E.H. Meijer, 2004b, Direct simulation of particle suspensions in a viscoelastic fluid in sliding bi-periodic frames, *J. Non-Newtonian Fluid Mech.* **121**, 15-33.

Hwang, W.R., M.A. Hulsen, H.E.H. Meijer and T.H. Kwon, 2004c, Direct numerical simulations of suspensions of spherical particles in a viscoelastic fluid in sliding tri-periodic domains, *Proceedings of the XIVth International Congress on Rheology* August 22-27, 2004; Editors: J.W. Lee and S.J. Lee, Seoul, Korea, CR10-1 to CR10-3.

Hwang, W.R., P.D. Anderson and M.A. Hulsen, 2005, Chaotic advection in a cavity flow with rigid particles, *Phys. Fluids* **17**, 043602-1--043602-12.

Hwang, W.R. and M.A. Hulsen, 2006, Direct numerical simulations of hard particle suspensions in planar elongational flow, *J. Non-Newtonian Fluid Mech.* **136**, 167-178.

Kraynik, A.M. and D.A. Reinelt, 1992, Extensional motions of spatially periodic lattices, *Intern. J. Multiphase Flow* **18**, 1045-1059.

Lees, A.W. and S.F. Edwards, 1972, The computer study of transport processes under extreme conditions, *J. Phys. C: Solid State Phys.* **5**, 1921-1929.

Mall-Gleissle, S.G., W. Gleissle, G.H. McKinley and H. Buggisch, 2002, The normal stress behaviour of suspensions with viscoelastic matrix fluids, *Rheol. Acta* **41**, 61-76.

Ohl, N. and W. Gleissle, 1993, The characterization of the steady-state shear and normal stress functions of highly concentrated suspensions formulated with viscoelastic liquids, *J. Rheol.* **37**, 381-406.

Patankar, N.A., P. Singh, D.D. Joseph, R. Glowinski and T.-W. Pan, 2000, A new formulation of the distributed Lagrangian

multipliers/fictitious domain method for particulate flows, *Intern. J. Multiphase Flow* **26**, 1509-1524.

Patankar, N.A. and H.H. Hu, 2001, Rheology of a suspension of particles in viscoelastic fluids, *J. Non-Newtonian Fluid Mech.* **96**, 423-443.

Schrauwen, B.A.G., L.E. Govaert, G.W.M. Peters and H.E.H. Meijer, 2002, The influence of flow-induced crystallization on the impact toughness of high-density polyethylene, *Macromol. Symp.* **185**, 89-102.

Seshaijer, P. and M. Suri, 2000, hp submeshing via non-conforming finite element methods, *Comput. Methods Appl. Mech. Engrg.* **189**, 1011-1030.

Sierou, A. and J.F. Brady, 2002, Rheology and microstructure in concetrated noncolloidal suspensions, *J. Rheol.* **46**, 1031-1056.

Tanaka, H. and J.L. White, 1980, Experimental investigations of shear and elongational flow properties of polystylene melts reinforced with calcium carbonate, titanium dioxide, and carbon black, *Polym. Eng. Sci.* **20**, 949-956.

Vermant, J. and M.J. Solomon, 2005, Flow-induced structure in colloidal suspensions, *J. Phys.: Condens. Matter* **17**, R187-R216

Yu, Z., N. Phan-Thien, Y. Fan and R.I. Tanner, 2002, Viscoelastic mobility problem of a system of particles, *J. Non-Newtonian Fluid Mech.* **104**, 87-124.